

Near-Infrared Luminescence from Visible-Light-Sensitized Hybrid Materials Covalently Linked with Tris(8-hydroxyquinolate)-lanthanide [Er(III), Nd(III), and Yb(III)] Derivatives

Lining Sun,^{*,†} Song Dang,[‡] Jiangbo Yu,[‡] Jing Feng,[‡] Liyi Shi,[†] and Hongjie Zhang^{*,‡}

Research Center of Nano Science and Technology, Shanghai University, Shanghai 200444, People's Republic of China, and State Key Laboratory of Rare Earth Resource Utilization, Changchun Institute of Applied Chemistry, Chinese Academy of Sciences, Changchun 130022, People's Republic of China

Received: September 17, 2010

A series of new near-infrared (NIR) luminescent lanthanide–quinolate derivatives [Ln(Q–Si)₃] and xerogels (named as LnQSi–Gel, Ln = Er, Nd, Yb) covalently linked with the Ln(Q–Si)₃ by using the 8-hydroxyquinoline-functionalized alkoxysilane (Q–Si) have been synthesized. The obtained xerogel materials LnQSi–Gel are rigid and show homogeneous by field-emission scanning electron microscopy (FE-SEM) images. The Fourier-transform infrared (FT-IR), fluorescence spectra of Ln(Q–Si)₃, and LnQSi–Gel were measured, and the corresponding luminescence decay analyses were recorded. Of importance here is that the excitation spectra of the Ln(Q–Si)₃ and LnQSi–Gel extend to the region of visible light (more than 500 nm). Upon ligand-mediated excitation with the visible light, the Ln(Q–Si)₃ and LnQSi–Gel show the characteristic NIR-luminescence of the corresponding lanthanide ions through the intramolecular energy transfer from the ligands to the lanthanide ions. The good luminescent performances enable these NIR-luminescent xerogel materials to have possible applications in medical diagnostics, laser systems, and optics, etc.

1. Introduction

Materials incorporating lanthanide ions (e.g., Nd³⁺, Er³⁺, Yb³⁺) are of great interest for a wide range of near-infrared (NIR) optical applications, such as laser systems,^{1–3} amplifiers for optical communication,^{4–6} and fluorescent bimolecular labeling in bioassays.^{7,8} Lanthanide ions exhibit, however, low luminescence intensity due to the fact that the 4f–4f transitions are parity forbidden. One of the most useful strategies that has been employed to overcome this drawback is the complexation of the lanthanide ions through the coordination with organic ligands acting as sensitizers, which is the so-called “antenna effect”.^{9,10} The ligands absorb UV or visible light and efficiently transfer the energy to the central lanthanide ion (intramolecular energy transfer), ultimately resulting in sensitized Ln³⁺ ion emission.

Most investigations have focused on organic ligands such as diketones, quinolines, phenanthrolines, cryptands, etc.^{2,11} 8-Hydroxyquinoline (HQ) and its metalloquinolates possess superb ability to chelate many metal ions and have been proved to be a suitable complexing agent for trivalent lanthanide ions.^{12,13} NIR-emitting lanthanide chelates based on HQ and its metalloquinolates have appeared frequently in recent literature, because they are promising candidates for active components in NIR-luminescent optical devices.^{14–16}

However, the practical applications of the NIR-luminescent lanthanide complexes are limited to a large extent, essentially due to their poor thermal stabilities and low mechanical strength.^{17,18} In the past few years, it has been recognized that the combination of the lanthanide complexes and inorganic networks with favorable thermal and mechanical characteristics

by using versatile sol–gel synthetic route allows these drawbacks to be successfully circumvented.^{10,19} Sol–gel-derived hybrid materials combine chemical and thermal stability, the mechanical strength and the process flexibility of silica, together with the functional characteristics of active organic molecules.^{20,21} Physical mixing of the lanthanide complexes into the sol–gel materials is very easy to do; however, the interactions between lanthanide complexes and silica moieties in such sol–gel hybrid materials are so weak that the phase separation, inhomogeneous dispersion, and optical quenching of the dopants may occur.^{22,23} To overcome these shortages, the HQ was functionalized with organosilane (the obtained alkoxysilane is named as Q–Si),²⁴ which can play double roles of not only coordinating with lanthanide ions but also acting as an organosilane precursor to synthesize the xerogel hybrid materials. The hydrolysis and polycondensation processes of the multifunctional alkoxysilane Q–Si and TEOS are easily controlled. Thus, the lanthanide quinolate derivatives can be covalently bonded to the xerogel material, and the problems mentioned above (phase separation and inhomogeneous dispersion between organic and inorganic moieties) can be avoided effectively. To the best of our knowledge, NIR-luminescence of the lanthanide complexes covalently linked xerogel via excitation into visible region have not been reported by other groups up until now.

Normally, the materials containing the lanthanide derivatives can be excited by ultraviolet light; however, materials excited with visible light are advantageous over ultraviolet-excitability materials for the reasons that (i) the long-wave excitation strongly reduces the background fluorescence, and (ii) the visible excitation is less prone to the interferences by inner filter effects due to the absorption of light, etc.^{25,26} In the present work, the new lanthanide–quinolate derivatives [Ln(Q–Si)₃] and xerogel materials covalently linked with lanthanide–quinolate derivatives [LnQSi–Gel, Ln = Er, Nd, Yb] by 8-hydroxyquino-

^{*} To whom correspondence should be addressed. E-mail: lnsun@shu.edu.cn (L.-N.S.); hongjie@ciac.jl.cn (H.-J.Z.).

[†] Shanghai University.

[‡] Changchun Institute of Applied Chemistry.

line-functionalized alkoxy silane (Q-Si) were synthesized. The xerogel materials were very rigid, and no cracks were observed. Upon excitation with the visible light, both the derivatives and the xerogel materials show the characteristic NIR-luminescence of the corresponding lanthanide ions. The NIR-luminescence behavior has been investigated in detail.

2. Experimental Section

2.1. Materials. Tetraethoxysilane (TEOS, Aldrich), (3-aminopropyl)triethoxysilane (APTES, Aldrich), sodium hydroxide, chloroform, and light petroleum were used as received. 8-Hydroxyquinoline (HQ, C. P.) was bought from Beijing Fine Chemical Co. (Beijing, China). Ytterbium oxide (Yb_2O_3 , 99.99%), neodymium oxide (Nd_2O_3 , 99.99%), and erbium oxide (Er_2O_3 , 99.99%) were purchased from Yue Long Chemical Plant (Shanghai, China).

Hydrated LnCl_3 salts ($\text{Ln} = \text{Er, Nd, Yb}$) were obtained by dissolving Ln_2O_3 in hydrochloric acid (HCl) and removing the surplus HCl by evaporation.

2.2. Synthesis of 8-Hydroxyquinoline-Functionalized Alkoxy-silane (Q-Si).²³ The method used for the synthesis of Q-Si was according to the reported procedure.²² The synthesis of 5-formyl-8-hydroxyquinoline was according to the literature and was characterized by the reported procedure.²⁷ The ethanol in this procedure was used after desiccation. The 5-formyl-8-hydroxyquinoline was dissolved in a suitable volume of anhydrous ethanol, and APTES was added with a molar ratio of 1:1 (APTES to 5-formyl-8-hydroxyquinoline), then refluxed for 12 h under stirring in a nitrogen atmosphere. Next, the solvent was distilled off under reduced pressure, yielding the 8-hydroxyquinoline-functionalized alkoxy silanes, Q-Si: a deep orange oil-like liquid (Q-Si). Anal Calcd for $\text{C}_{19}\text{H}_{28}\text{N}_2\text{O}_4\text{Si}$: C, 60.61%; H, 7.50%; N, 7.44%. Found: C, 60.12%; H, 7.62%; N, 7.84%. NMR (CDCl_3): δ 9.76 (1H, d); 8.80 (1H, d); 8.59 (1H, s); 7.68 (1H, d); 7.53 (1H, q); 7.18 (1H, d); 3.84 (6H, q); 3.66 (2H, t); 1.89 (2H, m); 1.23 (9H, t); 0.75 (2H, t).

2.3. Synthesis of Lanthanide Quinolate Derivatives [$\text{Ln}(\text{Q-Si})_3$, $\text{Ln} = \text{Er, Nd, Yb}$]. The Q-Si was dissolved in a suitable volume of anhydrous ethanol. A stoichiometric amount of lanthanide chloride ethanol solution was then added dropwise to the solution under stirring. The molar ratio of Ln^{3+} ion:Q-Si was 1:3. The orange-yellow precipitates (the colors are a little different depending on the lanthanide ions) appeared immediately. After being stirred for 4 h, they were collected by filtration and dried at 70 °C under vacuum overnight. Next, the precipitates were washed with anhydrous ethanol three times.

Elemental Analysis. Anal. Calcd for $\text{Er}(\text{Q-Si})_3$: C, 52.91%; H, 6.27%; N, 6.50%. Found: C, 52.05%; H, 6.02%; N, 6.29%. Anal. Calcd for $\text{Nd}(\text{Q-Si})_3$: C, 53.87%; H, 6.38%; N, 6.62%. Found: C, 52.97%; H, 6.10%; N, 6.38%. Anal. Calcd for $\text{Yb}(\text{Q-Si})_3$: C, 52.68%; H, 6.24%; N, 6.47%. Found: C, 51.89%; H, 6.09%; N, 6.21%.

2.4. Synthesis of the Xerogel Materials Covalently Linked with Lanthanide Quinolate Derivatives [LnQSi-Gel , $\text{Ln} = \text{Er, Nd, Yb}$]. Q-Si was dissolved in anhydrous ethanol, and then TEOS and deionized water (acidified with HCl, pH = 2) were added under stirring. After 2 h, an appropriate amount of LnCl_3 ethanol solution was introduced into the above solution. The molar ratio of Q-Si:TEOS: H_2O : Ln^{3+} was 3:75:300:1. The mixed solution was stirred for about 5 h at room temperature to ensure homogeneous mixing and achieve one single phase, and then placed into a cuvette. The precursor solution converted to a wet gel after several days of gelation at 40 °C and then was continuously dried to obtain a transparent xerogel. The

lanthanide-quinolate derivatives were supposed to be synthesized during the corresponding sol-to-xerogel conversion accompanied with the evaporation of HCl, respectively. For the luminescence and SEM measurements, the xerogel samples were ground to powders. The powders were then washed with water and ethanol for removal of the surplus Ln^{3+} ions; thus, all of the complexes in the materials were attached to the matrix by the Q-Si. Before the fluorescence measurements were operated, the materials were dried under a vacuum at 80 °C for 24 h.

2.5. Characterization. All measurements were carried out at room temperature. Scanning electron micrographs (SEM) were obtained using a JSM-6700F microscope operating at 10.0 kV. FT-IR spectra were measured within a 4000–400 cm^{-1} region on an American BIO-RAD Co. model FTS135 infrared spectrophotometer with the KBr pellet technique. The CHN elemental analyses were carried out on a VarioEL analyzer. The excitation and emission spectra were recorded by a HORIBA Jobin Yvon FluoroLog-3 spectrofluorometer equipped with a 450 W Xe-lamp as an excitation source and a monochromator iHR320 equipped with a liquid-nitrogen-cooled R5509-72 PMT as the detector. The time-resolved measurements were done by using the third harmonic (355 nm) of a Spectra-physics Nd:YAG laser with a 5 ns pulse width and 5 mJ of energy per pulse as the source, and the NIR emission lines were dispersed by a HORIBA Jobin Yvon emission monochromator iHR320 equipped with liquid-nitrogen-cooled R5509-72 PMT, and the data were analyzed with a LeCroy WaveRunner 6100 1 GHz Oscilloscope.

3. Results and Discussion

To obtain stable lanthanide complexes with good optical properties, the ligands are designed to provide enough coordination sites to bind the central ion, to shield it from the surrounding matrix, and also to act as “antenna chromophores” to transfer excitation energy to the central ion.²⁸ Figure S1 shows the structures of the $\text{Ln}(\text{Q-Si})_3$, which was predicted on the basis of the experimental process and the complex structure derived from HQ.^{29,30}

In silica-based sol-gel hybrid materials, there are numerous hydroxyl groups (in Si-OH and H_2O) that act as nonradiative channels for the excited states of the lanthanide ions and have strong quenching properties toward the luminescence of lanthanide complexes. In this case, the co-condensation of TEOS and Q-Si is able to induce some -OH groups to be substituted by organic groups; thus, the increased hydrophilicity of the modified materials can be achieved. Therefore, the Q-Si plays three roles during the sol-gel process: one is as an organosilane precursor to occur the cohydrolysis and copolycondensation with TEOS, the second is acting as a ligand to coordinate with the central lanthanide ions, and the third is acting a silylation agent for the precursor in the sol-gel process. In this way, the lanthanide quinolate derivatives were supposed to be synthesized and coupled to the silica backbone.³¹ The proposed structure of the LnQSi-Gel hybrid material is displayed in Scheme 1.

3.1. Fourier Transform Infrared Spectra (FT-IR). The FT-IR spectra of the $\text{Ln}(\text{Q-Si})_3$ and LnQSi-Gel hybrid materials have been measured and exhibit very similar results depending on different lanthanide ions, respectively. Figure 1 displays the representative patterns of $\text{Nd}(\text{Q-Si})_3$ and NdQSi-Gel . The band at 1641 cm^{-1} assigned to the C=N bond can be observed in Figure 1a and b, which suggests the retaining of the imine groups in the $\text{Nd}(\text{Q-Si})_3$ and NdQSi-Gel .²² After lanthanide-quinolate derivatives are covalently linked to the sol-gel,

SCHEME 1: Proposed Structure of the LnQSi-Gel, Ln = Er, Nd, Yb

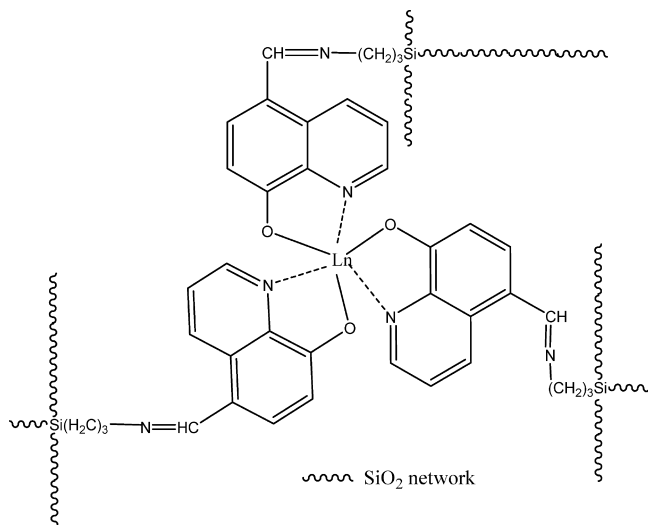


Figure 1b shows a different pattern from Figure 1a due to the hydrolysis/condensation of TEOS and Q-Si. In Figure 1b, the peak at 1080 cm^{-1} corresponds to the Si-O symmetric stretching vibration, and the band at 450 cm^{-1} can be attributed to the bending vibration of Si-O-Si band, which indicates the formation of the Si-O-Si framework in NdQSi-Gel.

3.2. Scanning Electron Microscopy (SEM). The LnQSi-Gel materials were transparent and rigid, and no cracks were observed. The SEM images of LnQSi-Gel (Ln = Er, Nd, and Yb) are very similar to each other, as shown by the representative pattern of the NdQSi-Gel. As shown in Figure 2, it can be observed that the NdQSi-Gel appears very homogeneous and no sign of any phase separation was observed even if the magnification was increased to 35 000. This can be explained by the strong covalent-bond bridge between the inorganic and organic phases.^{18,32} As a result, the material is composed quite uniformly and is one-component organic-inorganic hybrid material.³³

3.3. Photoluminescence Studies. Yb^{3+} ion is a very unusual case of the lanthanide ions, as it has only one single excited state, $^2\text{F}_{5/2}$, whose energy level is $10\,200\text{ cm}^{-1}$ above the $^2\text{F}_{7/2}$ ground state. Figure S2 and Figure 3 show the excitation and emission spectra of $\text{Yb}(\text{Q-Si})_3$ and YbQSi-Gel, respectively. The two excitation spectra both monitored at 980 nm are composed of a broad band in the ultraviolet/visible spectral range

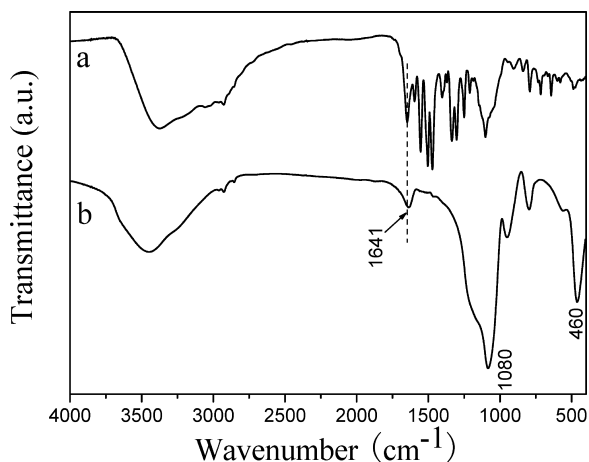


Figure 1. FT-IR spectra of (a) $\text{Nd}(\text{Q-Si})_3$ and (b) NdQSi-Gel.

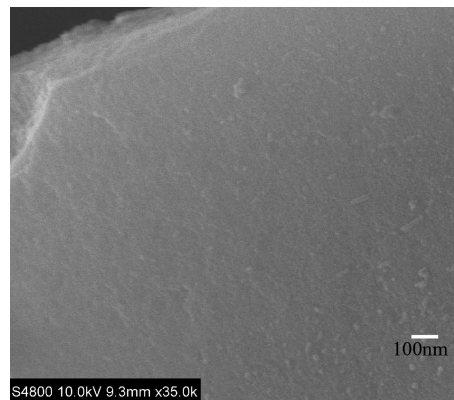


Figure 2. SEM images of NdQSi-Gel with a magnification of 35 000.

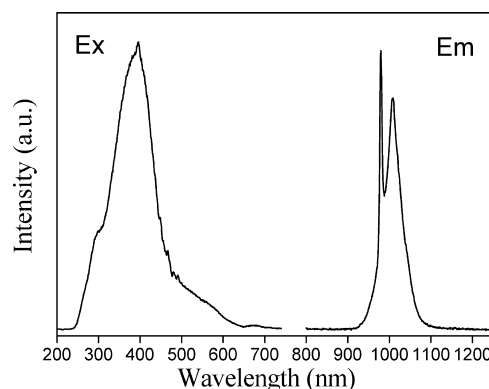


Figure 3. Excitation ($\lambda_{\text{em}} = 980\text{ nm}$) and emission ($\lambda_{\text{ex}} = 401\text{ nm}$) spectra for the YbQSi-Gel material.

from 240 to 650 nm , which is due to the light absorption by the organosilane Q-Si ligand. These broad bands extend to the visible range, which enables photoexcitation of $\text{Yb}(\text{Q-Si})_3$ and YbQSi-Gel by visible sources. After ligand-mediated excitation at 401 nm , both the emission spectra of the $\text{Yb}(\text{Q-Si})_3$ and YbQSi-Gel show the characteristic emission of the Yb^{3+} ion, a band in the $910\text{--}1180\text{ nm}$ range with the main and strongest peak at 980 nm . This is assigned to the $^2\text{F}_{5/2} \rightarrow ^2\text{F}_{7/2}$ transition of the Yb^{3+} ion.^{16,18,23} It should also be noted that the Yb^{3+} ion emission band is not a single sharp band but a shoulder peak arising at long wavelength than the primary 980 nm peak. Similar splitting has been reported previously, and this may be due to the splitting of the energy levels of the Yb^{3+} ion as a consequence of ligand field effects.³⁴ It was reported that the Yb^{3+} ion has some advantages for laser emission because of its very simple f-f energy level structure mentioned above.^{18,35} In addition, the relative transparency of human tissue at approximately 1000 nm suggests that in vivo luminescent probes operating at this wavelength (Yb^{3+} ion-based emission) could have diagnostic value. Thus, the visible-light-sensitized $\text{Yb}(\text{Q-Si})_3$ and YbQSi-Gel have potential application in laser systems and medical diagnostic.

The fluorescence spectra of $\text{Nd}(\text{Q-Si})_3$ and NdQSi-Gel are shown in Figure S3 and Figure 4, respectively. The excitation spectra were obtained by monitoring the strongest emission of the Nd^{3+} ion at 1064 nm . For $\text{Nd}(\text{Q-Si})_3$ and NdQSi-Gel, the broad bands ranging from $227\text{ to }643\text{ nm}$ and from $237\text{ to }605\text{ nm}$ of the excitation spectra can be observed, respectively, which is assigned to the absorption of the Q-Si ligand, superimposed with the excitation band (at 581 nm) originating from the characteristic absorption transition $^4\text{I}_{9/2} \rightarrow ^2\text{G}_{7/2}$ of the Nd^{3+} ion. It should be noted that the absorption transition at 581 nm

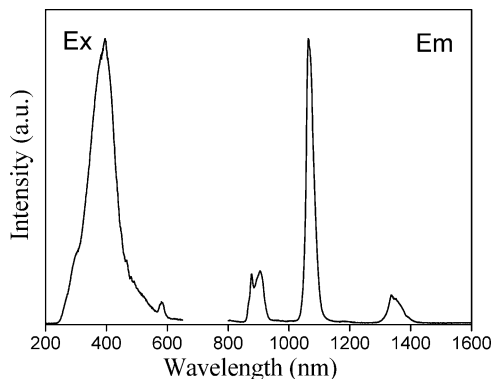


Figure 4. Excitation ($\lambda_{em} = 1064$ nm) and emission ($\lambda_{ex} = 401$ nm) spectra for the NdQSi-Gel material.

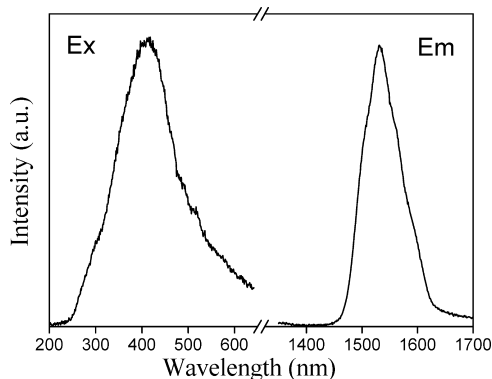


Figure 5. Excitation ($\lambda_{em} = 1531$ nm) and emission ($\lambda_{ex} = 415$ nm) spectra for the ErQSi-Gel material.

of the Nd^{3+} ion is much weaker than that of the ligand, which shows that the luminescence sensitization via exciting the ligand is much more efficient than directly exciting the absorption level of the Nd^{3+} ion. Following the photoexcitation at 401 nm, the characteristic Nd^{3+} ion emissions were obtained for $\text{Nd}(\text{Q-Si})_3$ and NdQSi-Gel. Both of the two emission spectra consist of three bands, peaking at 904, 1064, and 1338 nm for $\text{Nd}(\text{Q-Si})_3$, and peaking at 905, 1064, and 1336 nm for NdQSi-Gel. They can be attributed to the f-f transitions of $^4\text{F}_{3/2} \rightarrow ^4\text{I}_{9/2}$, $^4\text{F}_{3/2} \rightarrow ^4\text{I}_{11/2}$, and $^4\text{F}_{3/2} \rightarrow ^4\text{I}_{13/2}$, respectively. Among the three emission bands of the two emission spectra, the band centered at 1064 nm shows the strongest intensity, which is potentially applicable for the laser system.^{36,37}

Figure S4 and Figure 5 display the excitation and emission spectra of $\text{Er}(\text{Q-Si})_3$ and ErQSi-Gel, respectively. The broad bands extending to more than 600 nm of the two excitation spectra are due to the absorption of the organosilane Q-Si. Upon excitation of the ligand absorption at 401 and 415 nm, the emission spectra of $\text{Er}(\text{Q-Si})_3$ and ErQSi-Gel were obtained, centered at 1533 and 1531 nm, respectively. The emission bands cover large spectrum ranges, and extend from 1425 to 1660 nm for $\text{Er}(\text{Q-Si})_3$ and from 1430 to 1700 nm for ErQSi-Gel, respectively, which are attributed to the transition from the first excited state to the ground state ($^4\text{I}_{13/2} \rightarrow ^4\text{I}_{15/2}$) of the Er^{3+} ion. For a long time, the erbium-doped materials have attracted much attention in the field of optical amplification because the transition around $1.54 \mu\text{m}$ matches one of the fiber low-loss windows well and is in the right position of the third telecommunication window. To enable a wide gain bandwidth for optical amplification, a broad emission band of this transition is desirable.⁶ In this case, the full width at half-maximum (fwhm) values of the $^4\text{I}_{13/2} \rightarrow ^4\text{I}_{15/2}$ transition for $\text{Er}(\text{Q-Si})_3$ and ErQSi-Gel are 82 and 81 nm, respectively. In comparison with

other Er-doped materials, the fwhms of $\text{Er}(\text{Q-Si})_3$ and ErQSi-Gel are quite broad, which is necessary for getting a wide gain bandwidth for optical amplification.^{18,38,39}

As described above, the characteristic NIR-emission of Ln^{3+} ion was obtained in the corresponding $\text{Ln}(\text{Q-Si})_3$ and LnQSi-Gel ($\text{Ln} = \text{Er}, \text{Nd}, \text{Yb}$) material by exciting the visible-light-absorption of the organic ligands, respectively. The observed NIR emissions do arise by the sensitization of the lanthanide ions from the organic ligands moiety, because no absorption of the lanthanide ions occurs at the corresponding excitation wavelengths. Thus, it is obvious that the intramolecular energy transfer does happen between the organic ligands and the lanthanide ions. Therefore, it is reasonable to conclude that the lanthanide complexes are synthesized and covalently linked to the silica network in the LnQSi-Gel (Scheme 1). The triplet-state energy level of Q-Si ligand is determined to be $21\,090 \text{ cm}^{-1}$ from the phosphorescence spectrum of the corresponding Gd complex at 77 K.²⁴ According to Dexter's theory,⁴⁰ the Q-Si ligand can match well with the 4f levels of the Ln^{3+} ions, and the efficient NIR luminescence of the Ln^{3+} ions can be obtained in the corresponding $\text{Ln}(\text{Q-Si})_3$ and LnQSi-Gel ($\text{Ln} = \text{Er}, \text{Nd}, \text{Yb}$) materials, respectively.

The lifetime measurement of $\text{Ln}(\text{Q-Si})_3$ and LnQSi-Gel ($\text{Ln} = \text{Er}, \text{Nd}, \text{Yb}$) was investigated by using an excitation wavelength of 355 nm and monitored around the strongest emission line of their corresponding emission spectra. The decays of $\text{Ln}(\text{Q-Si})_3$ are single-exponential, and the corresponding lifetimes of the $^2\text{F}_{5/2} \rightarrow ^2\text{F}_{7/2}$ transition of $\text{Yb}(\text{Q-Si})_3$, $^4\text{F}_{3/2} \rightarrow ^4\text{I}_{11/2}$ transition of $\text{Nd}(\text{Q-Si})_3$, and $^4\text{I}_{13/2} \rightarrow ^4\text{I}_{15/2}$ transition of $\text{Er}(\text{Q-Si})_3$ complexes are 1.9, 0.14, and 0.48 μs , respectively. The decay curve for NdQSi-Gel is singly exponential, and the corresponding lifetime of the $^4\text{F}_{3/2} \rightarrow ^4\text{I}_{11/2}$ transition is 75 ns. The decay curves for YbQSi-Gel and ErQSi-Gel can be fitted by the double-exponential function. The lifetimes of the $^2\text{F}_{5/2} \rightarrow ^2\text{F}_{7/2}$ transition of Yb^{3+} ion are 1.20 μs (56.5%) and 0.36 μs (43.5%). The lifetimes of the $^4\text{I}_{13/2} \rightarrow ^4\text{I}_{15/2}$ transition of Er^{3+} ion are 0.11 μs (48.1%) and 0.62 μs (51.9%).

4. Conclusions

The lanthanide quinolate derivatives $\text{Ln}(\text{Q-Si})_3$ have been synthesized and covalently bonded to xerogel by using the 8-hydroxyquinoline-functionalized alkoxy silane Q-Si successfully. The xerogels LnQSi-Gel ($\text{Ln} = \text{Er}, \text{Nd}, \text{Yb}$) appear very homogeneous with no sign of any phase separation as shown by SEM image. Following the visible-light excitation, the characteristic NIR-luminescence properties of $\text{Ln}(\text{Q-Si})_3$ and LnQSi-Gel ($\text{Ln} = \text{Er}, \text{Nd}, \text{Yb}$) show that the ligands shield the lanthanide ions well from their surroundings and efficiently transfer energy from their triplet states to the lanthanide ions. The good NIR-luminescent properties of the LnQSi-Gel hybrid materials upon excitation with the visible light provide an access to multicomposite in optical applications, such as in medical diagnostic probe, lasers, and optical amplifications.

Acknowledgment. We are grateful for the financial support from the National Natural Science Foundation of China (Grant Nos. 21001072 and 20771099) and the MOST of China (Grant No. 2006CB601103, 2006DFA42610), the Innovative Foundation of Shanghai University (A.10-0110-09-906), the Key Subject of the Municipal Educational Commission of Shanghai (project J50102), and the Special Project for Nanotechnology Shanghai (1052 nm03400).

Supporting Information Available: Structure of the $\text{Ln}(\text{Q}-\text{Si})_3$ complex ($\text{Ln} = \text{Er}, \text{Nd}, \text{Yb}$). Excitation and emission spectra for the $\text{Ln}(\text{Q}-\text{Si})_3$ complex ($\text{Ln} = \text{Er}, \text{Nd}, \text{Yb}$). This material is available free of charge via the Internet at <http://pubs.acs.org>.

References and Notes

- (1) Ryo, M.; Wada, Y.; Okubo, T.; Hasegawa, Y.; Yanagida, S. *J. Phys. Chem. B* **2003**, *107*, 11302.
- (2) Sun, L. N.; Zhang, H. J.; Meng, Q. G.; Liu, F. Y.; Fu, L. S.; Peng, C. Y.; Yu, J. B.; Zheng, G. L.; Wang, S. B. *J. Phys. Chem. B* **2005**, *109*, 6174.
- (3) Bassett, A. P.; Magennis, S. W.; Glover, P. B.; Lewis, D. J.; Spencer, N.; Parsons, S.; Williams, R. M.; De Cola, L.; Pikramenou, Z. *J. Am. Chem. Soc.* **2004**, *126*, 9413.
- (4) Sun, R. G.; Wang, Y. Z.; Zheng, Q. B.; Zhang, H. J.; Epstein, A. J. *J. Appl. Phys.* **2000**, *87*, 7589.
- (5) Mancino, G.; Ferguson, A. J.; Beeby, A.; Long, N. J.; Jones, T. S. *J. Am. Chem. Soc.* **2005**, *127*, 524.
- (6) Van Deun, R.; Nockemann, P.; Görrler-Walrand, C.; Binnemans, K. *Chem. Phys. Lett.* **2004**, *397*, 447.
- (7) Zhang, J.; Badger, P. D.; Geib, S. J.; Petoud, S. *Angew. Chem., Int. Ed.* **2005**, *44*, 2508.
- (8) Sun, L. N.; Yu, J. B.; Zheng, G. L.; Zhang, H. J.; Meng, Q. G.; Peng, C. Y.; Fu, L. S.; Liu, F. Y.; Yu, Y. N. *Eur. J. Inorg. Chem.* **2006**, 3962.
- (9) Bünzli, J.-C.; Piguet, C. *Chem. Soc. Rev.* **2005**, *34*, 1048.
- (10) Fernandes, M.; Nobre, S. S.; Gonçalves, M. C.; Charas, A.; Morgado, J.; Ferreira, R. A. S.; Carlos, L. D.; de Zea Bermudez, V. *J. Mater. Chem.* **2009**, *19*, 733.
- (11) (a) Artizzu, F.; Deplano, P.; Marchiò, L.; Mercuri, M. L.; Pillia, L.; Serpe, A.; Quochi, F.; Orrù, R.; Cordella, F.; Meinardi, F.; Tubino, R.; Mura, A.; Bongiovanni, G. *Inorg. Chem.* **2005**, *44*, 840. (b) Suzuki, H.; Hattori, Y.; Lizuka, T.; Yuzawa, K.; Matsumoto, N. *Thin Solid Films* **2003**, *39*, 288. (c) Oude Wolbers, M. P.; van Veggel, F. C. J. M.; Snellink-Ruël, B. H. M.; Hofstra, J. W.; Geurts, F. A. J.; Reinhoudt, D. N. *J. Am. Chem. Soc.* **1997**, *119*, 138.
- (12) Albrecht, M.; Ossetka, O.; Klankermayer, J.; Fröhlich, R.; Gummy, F.; Bünzli, J.-C. G. *Chem. Commun.* **2007**, 1834.
- (13) Khreis, O. M.; Curry, R. J.; Somerton, M.; Gillin, W. P. *J. Appl. Phys.* **2000**, *88*, 777.
- (14) Van Deun, R.; Fias, P.; Nockemann, P.; Van Hecke, K.; Van Meervelt, L.; Binnemans, K. *Eur. J. Inorg. Chem.* **2007**, 302.
- (15) Artizzu, F.; Deplano, P.; Marchiò, L.; Mercuri, M. L.; Pillia, L.; Serpe, A.; Quochi, F.; Orrù, R.; Cordella, F.; Meinardi, F.; Tubino, R.; Mura, A.; Bongiovanni, G. *Inorg. Chem.* **2005**, *44*, 840.
- (16) Comby, S.; Imbert, D.; Vandevyver, C.; Bünzli, J.-C. G. *Chem.-Eur. J.* **2007**, *13*, 936.
- (17) Sanchez, C.; Lebeau, B.; Chaput, F.; Boilot, J. P. *Adv. Mater.* **2003**, *15*, 1969.
- (18) Sun, L. N.; Zhang, H. J.; Yu, J. B.; Meng, Q. G.; Liu, F. Y.; Peng, C. Y. *J. Photochem. Photobiol., A* **2008**, *193*, 153.
- (19) Sun, L. N.; Zhang, H. J.; Fu, L. S.; Liu, F. Y.; Meng, Q. G.; Peng, C. Y.; Yu, J. B. *Adv. Funct. Mater.* **2005**, *15*, 1041.
- (20) Sanchez, C.; Soler-Illia, G. J. A. A.; Ribot, F.; Lalot, T.; Mayer, C. R.; Cabuil, V. *Chem. Mater.* **2001**, *13*, 3061.
- (21) Corriu, R. J. P.; Embert, F.; Guari, Y.; Mehdi, A.; Reyé, C. *Chem. Commun.* **2001**, 1116.
- (22) Zeng, H. Y.; Huang, W. M.; Shi, J. L. *Chem. Commun.* **2006**, 880.
- (23) Binnemans, K. In *Handbook on the Physics and Chemistry of Rare Earths*; Gschneidner, K. A., Jr.; Bünzli, J.-C. G., Pecharsky, V. K., Eds.; Elsevier: Amsterdam, 2005; Vol. 35, Chapter 225, pp 107–272.
- (24) Sun, L. N.; Zhang, H. J.; Yu, J. B.; Yu, S. Y.; Peng, C. Y.; Dang, S.; Guo, X. M.; Feng, J. *Langmuir* **2008**, *24*, 5500.
- (25) Peng, H.; Stich, M. I. J.; Yu, J.; Sun, L. N.; Fischer, L. H.; Wolfbeis, O. S. *Adv. Mater.* **2010**, *22*, 716.
- (26) Yang, C.; Fu, L. M.; Wang, Y.; Zhang, J. P.; Wong, W. T.; Ai, X. C.; Qiao, Y. F.; Zhou, B. S.; Gui, L. L. *Angew. Chem., Int. Ed.* **2004**, *43*, 5009.
- (27) Clemon, G. R.; Howe, R. J. *Chem. Soc.* **1955**, 3552.
- (28) Song, L.; Wang, Q.; Tang, D.; Liu, X.; Zhen, Z. *New J. Chem.* **2007**, *31*, 506.
- (29) Gillin, W. P.; Curry, R. J. *Appl. Phys. Lett.* **1999**, *74*, 798.
- (30) Khreis, O. M.; Curry, R. J.; Somerton, M.; Gillin, W. P. *J. Appl. Phys.* **2000**, *88*, 777.
- (31) Sui, Y. L.; Yan, B. *J. Photochem. Photobiol., A* **2006**, *182*, 1.
- (32) Cui, Y. J.; Qian, G. D.; Gao, J. K.; Chen, L. J.; Wang, Z. Y.; Wang, M. Q. *J. Phys. Chem. B* **2005**, *109*, 23295.
- (33) Wang, Q. M.; Yan, B. *J. Mater. Chem.* **2004**, *14*, 2450.
- (34) Wolbers, M. P. O.; van Veggel, F. C. J. M.; Snellink-Ruël, B. H. M.; Hofstra, J. W.; Geurts, F. A. J.; Reinhoudt, D. N. *J. Chem. Soc., Perkin Trans. 2* **1998**, 2141.
- (35) Boulon, G.; Collombet, A.; Brenier, A.; Cohen-Adad, M. T.; Yoshikawa, A.; Lebbou, K.; Lee, J. H.; Fukuda, T. *Adv. Funct. Mater.* **2001**, *11*, 263.
- (36) Klink, S. I.; Alink, P. O.; Grave, L.; Peters, F. G. A.; Hofstra, J. W.; Geurts, F.; van Veggel, F. C. J. M. *J. Chem. Soc., Perkin Trans. 2* **2001**, 363, 40.
- (37) Lai, W. P.-W.; Wong, W.-T. *New J. Chem.* **2000**, *24*, 943.
- (38) Polman, A.; van Veggel, F. C. J. M. *J. Opt. Soc. Am. B* **2004**, *21*, 871.
- (39) Park, O. H.; Seo, S. Y.; Jung, J. I.; Bae, J. Y.; Bae, B. S. *J. Mater. Res.* **2003**, *18*, 1039.
- (40) Dexter, D. L. *J. Chem. Phys.* **1953**, *21*, 836.

JP1088993